



# Benign Hepatic Neoplasms: An Imaging Review

Rajendra Kumar Behera<sup>1</sup> Stuti Chandola<sup>1</sup> Ankur Goyal<sup>1</sup>  Raju Sharma<sup>1</sup>

<sup>1</sup>Department of Radiodiagnosis and Interventional Radiology, All India Institute of Medical Sciences, New Delhi, India

Address for correspondence Raju Sharma, MD, MAMS, FICR, Department of Radiodiagnosis and Interventional Radiology, All India Institute of Medical Sciences, Sri Aurobindo Marg, Ansari Nagar, New Delhi 110029, India (e-mail: raju152@yahoo.com).

J Gastrointestinal Abdominal Radiol ISGAR 2023;6:109–122.

## Abstract

Benign liver neoplasms are commonly encountered in clinical practice. Lesions like typical hemangioma may be confidently diagnosed on ultrasound, but for the majority of other liver lesions, multiphasic computed tomography (CT) and magnetic resonance imaging (MRI) are usually warranted. In lesions like adenomas, making the diagnosis alone is not sufficient; rather subcategorization is important to optimally manage these cases. Additionally, commonly observed variant lesions like the inflammatory subtype of hepatocellular adenoma and focal nodular hyperplasia mimic each other, which exacerbates the diagnostic dilemma. When observing cystic lesions, mucinous cystic neoplasm of the liver (MCN-L) needs to be differentiated from the more common non-neoplastic etiologies like hydatid cysts. Radiologists should also be acquainted with features of rare hepatic neoplasms like angiomyolipoma, paraganglioma, and inflammatory pseudotumor. In this review, we discuss the salient features and differentiating points to suggest the most likely diagnosis.

## Keywords

- ▶ benign liver lesions
- ▶ hepatocellular adenoma
- ▶ focal nodular hyperplasia
- ▶ mucinous cystic neoplasms
- ▶ liver

## Introduction

Focal lesions in the liver are a common clinical problem and a significant proportion of these are benign, particularly those which are detected incidentally. In most cases, characteristic imaging appearance may enable noninvasive diagnosis. Occasionally, atypical and overlapping imaging features can lead to a diagnostic conundrum. While computed tomography (CT) remains the workhorse for evaluation of focal liver lesions, magnetic resonance imaging (MRI) offers additional information, useful in characterization, and is thus preferred for focal liver lesions. The other challenge includes rarely observed masses, with little knowledge about their imaging features. It is therefore imperative for the radiologist to be aware of typical and atypical features of commonly encountered benign liver tumors on different imaging modalities.

Benign liver tumors are classified either according to their cell of origin or on the basis of morphological features encountered on contrast-enhanced cross-sectional imaging. The former

classification divides the tumors into tumors of hepatocellular, cholangiocellular, and mesenchymal origin. Morphologically, the lesions can be divided into those which display arterial phase hyperenhancement and those which do not. This review describes the benign hepatic tumors with an emphasis on the classification based on their histological origin.

### Tumors of Hepatocellular Origin

These neoplasms develop due to deranged development and proliferation of primitive hepatocytes and include hepatocellular adenoma (HCA), focal nodular hyperplasia, and regenerative nodules.

### Adenoma

HCAs are rare benign tumors of hepatocellular origin. HCAs are most often seen in females with a history of oral contraceptive (OCP) use. The other predisposing factors include anabolic steroid use in males and underlying glycogen storage disease.

article published online  
April 18, 2023

DOI <https://doi.org/10.1055/s-0043-1764378>.  
ISSN 2581-9933.

© 2023. The Author(s).

This is an open access article published by Thieme under the terms of the Creative Commons Attribution License, permitting unrestricted use, distribution, and reproduction so long as the original work is properly cited. (<https://creativecommons.org/licenses/by/4.0/>)

Thieme Medical and Scientific Publishers Pvt. Ltd., A-12, 2nd Floor, Sector 2, Noida-201301 UP, India

HCA are typically solitary (80%); however, multiple adenomas may develop in the setting of glycogen storage disease.<sup>1</sup> Pathologically, HCAs are well-circumscribed lesions with areas of hemorrhage and infarction. They are composed of well-differentiated hepatocytes without any bile ductal cells or portal triads. The risk of hemorrhage is due to large plates of cells separated by dilated sinusoids, only arterial supply without any portal venous supply and poor connective tissue support. HCAs can rarely undergo malignant transformation as well.<sup>2,3</sup>

HCAs are subgrouped into the following eight molecular subtypes: (1) hepatocyte nuclear factor 1 alpha (HNF-1 $\alpha$ ), (2) inflammatory, (3)  $\beta$ -catenin exon 3, (4)  $\beta$ -catenin exon 7/8, (5) sonic hedgehog, (6) mixed  $\beta$ -catenin exon 3 and inflammatory, (7) mixed  $\beta$ -catenin exon 7/8 and inflammatory, and (8) unclassified.<sup>4</sup> Relevant features of the various subtypes are tabulated in **Table 1**.

HCAs are usually asymptomatic and may present as increased inflammatory markers and abnormalities in liver function like in inflammatory HCAs. Risk of hemorrhage strongly correlates with the subtype ( $\beta$ -catenin exon 7/8 HCA and sonic hedgehog types showing the maximum association). The sonic hedgehog subtype, in particular, has shown significant increased risk of symptomatic bleeding.<sup>5</sup> Size of the tumor (>5 cm) is also associated with histological hemorrhage, but it fails to show a statistically significant association with symptomatic bleeding.<sup>4</sup> Risk of malignant transformation depends on the interplay of various factors including sex, clinical features, and genetics of the tumor. Predisposing features of malignant transformation include male sex, high alcohol intake, type 2 diabetes, and pathological features of fibrosis, cholestasis, and pseudoglandular formation, with the latter being associated with  $\beta$ -catenin activation. Tumor size, however, has not been shown to be associated with the risk of malignant transformation.<sup>4</sup>

Ultrasound (US) features of HCA are nonspecific and include a well-circumscribed heterogeneous echotexture lesion without lobulations. Contrast-enhanced US (CEUS) may show certain specific features, for example, the inflammatory subtype shows centripetal filling in and central washout, while the HNF-1 $\alpha$  subtype shows no washout. On noncontrast CT (NCCT), adenomas are relatively hypo- to isodense, show arterial phase hyperenhancement (APHE), and become iso-enhancing to the liver parenchyma on portal venous and delayed phase images.

MRI is the ideal imaging modality to distinguish between the subtypes of HCA because of its ability to demonstrate intravoxel fat and T2 signal. On MRI, HCAs show hyperintense signal on T1-weighted images due to hemorrhage, which is therefore not suppressed with fat saturation. These lesions show loss of signal in the opposed-phase images as compared with in-phase images due to the intracellular fat (characteristic in the HNF-1 $\alpha$  subtype; **Fig. 1**). Background liver parenchyma may also show diffuse fatty changes in addition to intralesional fat in HCAs. HCAs show heterogeneous hyperintense signal on T2-weighted (T2W) images (due to varying degrees of hemorrhage, necrosis, fat, and

rarely calcification). T2 hyperintensity is marked in the inflammatory subtype, especially in periphery, which correlates with the presence of sinusoidal dilatation on pathology. On postcontrast sequences, APHE is seen, which may or may not persist in the portal phase. While nonhemorrhagic lesions show diffuse homogeneous APHE, the presence of intralesional necrosis and bleed may result in heterogeneous enhancement. Lack of washout in portal venous and delayed phases helps differentiate these lesions from hepatocellular carcinoma (HCC), which also contains fat in 40% cases.<sup>4</sup> Usually, HCAs do not show any enhancement in the hepatobiliary phase (HBP) due to lack of uptake of hepatocyte-specific contrast agents. However, up to 20% cases may show persistent enhancement, which is especially observed in  $\beta$ -catenin-mutated HCAs.<sup>5,6</sup> Expression of the organic anion transporting polypeptide (OATP) B1 and B3 transporter proteins is mainly responsible for the uptake of hepatobiliary contrast agents, and  $\beta$ -catenin activation contributes to overexpression of OATPB1/B3, with subsequent intermediate to high signal intensity in the HBP.<sup>5</sup> Additionally, the inflammatory subtype of HCA may also show a central scar and enhancement in the HBP. Therefore, both variants may potentially mimic FNH.

The enhancement of HCA is classically described to progress from the periphery toward the center of the lesion and these dynamics may be appreciated on CEUS or digital subtraction angiography (DSA).<sup>6</sup>

The presence of 10 or more adenomas, involving both the lobes of the liver, is termed adenomatosis. Adenomatosis is associated with type 3 maturity-onset diabetes of the young (MODY3) and not associated with OCPs/androgens. These lesions usually show HNF-1 $\alpha$  gene mutations.

Management of a hepatic adenoma needs to be tailored with every patient and is based upon the clinical profile, lesion size, risk of hemorrhage, and malignant transformation (**Fig. 2**). In general, adenomas up to 5 cm in size can be kept on observation and follow-up, whereas those larger than 5 cm are resected due to the risk of hemorrhage.<sup>4</sup> Surgery is also indicated for smaller adenomas with histology showing subtypes having propensity to bleed or undergo malignant degeneration.

### Focal Nodular Hyperplasia

FNH is the second most common benign tumor of the liver after hemangioma. It has an incidence of 0.9%, is more common in women than in men (8:1), and occurs in the third to fifth decade of life. FNH is usually single; however, multiple lesions may be seen in 20% of cases.<sup>7</sup> FNH occurs as a hyperplastic response of hepatocytes to abnormal blood flow without normal development of the portal tract.<sup>8</sup> Bile ductules proliferate without communication with the biliary tree and Kupffer's cells are present in abundance. FNH are usually asymptomatic and incidentally detected on imaging and rarely symptomatic (secondary to mass effect). They have no risk of malignancy, and complications like hemorrhage and rupture are unusual.

FNH is a well-circumscribed, nonencapsulated mass, usually smaller than 5 cm in size. On US, FNH is difficult

**Table 1** Clinical and morphological features of various subtypes of hepatocellular adenomas (HCAs)

Subtype	Genetic mutation	Demographic features	Complications	Specific imaging features
HNF-1 $\alpha$	Inactivating mutations of hepatocyte nuclear factor 1 alpha (HNF-1 $\alpha$ )	Common in females, associated with adenomatosis	Lowest risk of hemorrhage	<i>CEUS</i> No washout on CEUS <i>MRI</i> Presence of intracellular fat: diffuse signal drop on T1-opposed phase Background liver steatosis <i>Postcontrast</i> Arterial: moderate enhancement Portal venous and delayed; no persistent enhancement
Inflammatory (telangiectatic)	Janus kinase (JAK)/signal transducer and activator of transcription (STAT) pathway activation; multiple other mutations	Associated with estrogen (OCP) exposure, glycogen storage disease	Association with hemorrhage	<i>CEUS</i> Arterial: centripetal filling in late venous—central washout <i>MRI</i> Marked T2 hyperintensity, more in periphery (due to sinusoidal dilatation) <i>Postcontrast</i> Persistence of enhancement in portal venous, delayed, and hepatobiliary phases (so mimics FNH)
$\beta$ -catenin exon 3	Mutation in cadherins, exon 3	More common in males, associated with androgen exposure	Increased risk of malignant transformation to HCC due to TERT promoter mutation and positive glutamine synthetase	<i>MRI</i> No T1- or T2-specific features <i>Postcontrast</i> Arterial: marked enhancement Portal venous and delayed; may show washout, therefore mimicking HCC Enhancement in hepatobiliary phases also described
$\beta$ -catenin exon 7/8	Weak $\beta$ -catenin mutation, activation of the Wnt/ $\beta$ -catenin pathway	Younger age	High association with hemorrhage	–
Sonic hedgehog	Activation of the sonic hedgehog pathway	–	High association with hemorrhage	–
Mixed $\beta$ -catenin exon 3 and inflammatory	Inflammatory phenotype and activating mutations of exon 3	–	–	–
Mixed $\beta$ -catenin exon 7/8 and inflammatory	Inflammatory phenotype and activating mutations of exon 7/8	–	–	–
Unclassified	–	–	–	–

Abbreviations: CEUS, contrast-enhanced ultrasound; FNH, focal nodular hyperplasia; HCC, hepatocellular carcinoma; MRI, magnetic resonance imaging; OCP, oral contraceptive; TERT, telomerase reverse transcriptase.

Note: MRI is the ideal imaging modality to distinguish between the subtypes of HCA.

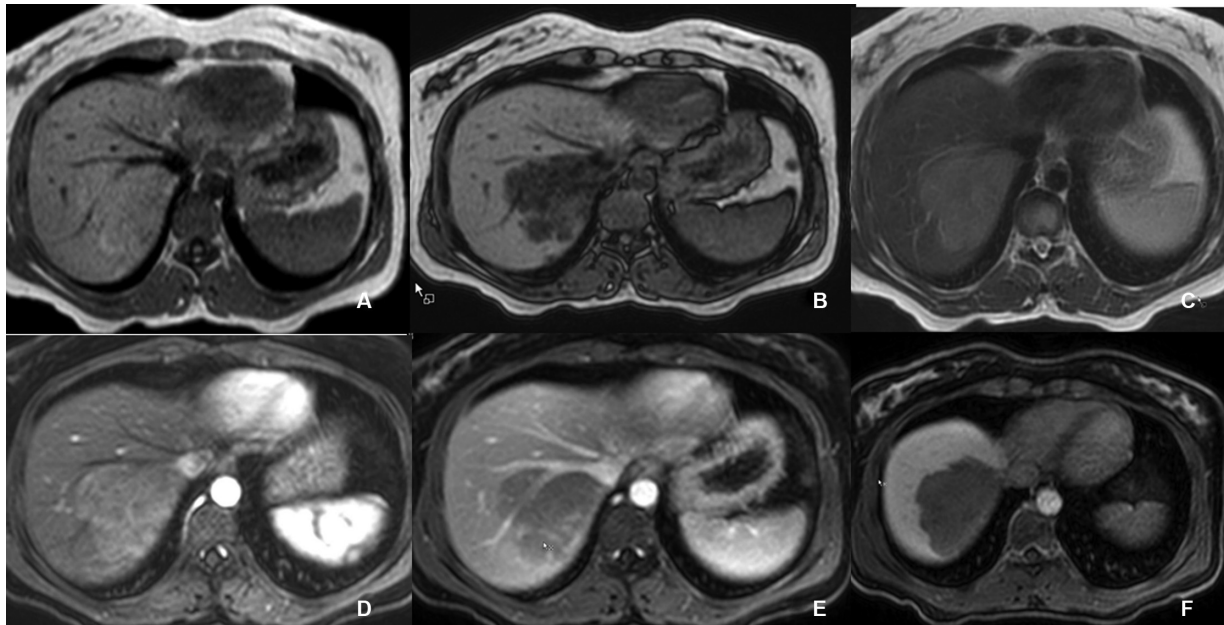


**Fig. 1** Hepatic adenoma in a 32-year-old woman with pain in the right hypochondrium. Axial T1-weighted (T1W) magnetic resonance (MR) images in in-phase (A) and (B) opposed phases demonstrate a well-margined mass in segments VIII and VII of the right lobe, which appears hyperintense to adjacent liver on T1 in phase with significant diffuse signal drop on opposed phase, suggesting intravoxel fat. (C) On axial T2W image, the lesion appears mildly hyperintense. Background liver shows normal outline. (D) Axial postcontrast image in arterial phase demonstrates homogeneous nonrim hyperenhancement within the lesion. It shows (E) washout without any significant contrast retention on the portal venous phase and (F) appears hypointense on the hepatobiliary phase. The MR features suggested steatotic hypervascular lesion and presence of hepatocyte nuclear factor 1 alpha (HNF-1 $\alpha$ ) mutation was subsequently confirmed on biopsy.

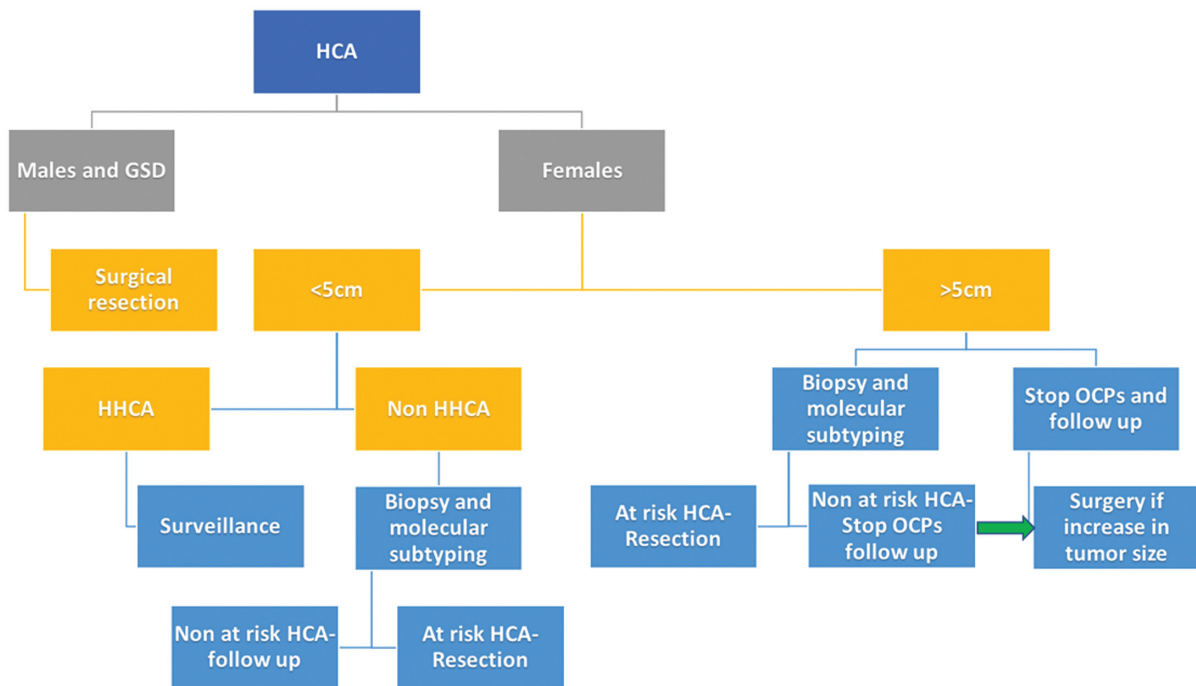


**Fig. 2** Management approach of an asymptomatic hepatocellular adenoma. GSD, glycogen storage disease; at-risk HCAs (hepatocellular adenomas):  $\beta$ -catenin exon 3, mixed  $\beta$ -catenin 3, and inflammatory HCA, sonic hedgehog subtype; non-at-risk HCA: HNF-1 $\alpha$  (hepatocyte nuclear factor 1 alpha), inflammatory,  $\beta$ -catenin 7/8, mixed  $\beta$ -catenin 7/8, and inflammatory, unclassified.)

to identify and may be iso- to hyperechoic and color Doppler may show central feeding artery. The lesion remains hypodense to the liver on unenhanced CT. Typical imaging features of FNH observed on noncontrast MR sequences include a T2-hyperintense central scar, which is also T1 hypointense and hyperintense on the ADC map. About 22% of lesions can show intralesional fat, and these steatotic varieties of FNH need to be differentiated from hepatic adenomas.<sup>9-12</sup>

On CEUS, CT, and MRI, FNH shows homogenous arterial phase hyperenhancement due to central feeding arterial supply.<sup>9</sup> Large feeding artery in the central scar is best demonstrated in the early arterial phase and therefore is usually not visualized as routinely late arterial phase is acquired. The lesion remains iso-enhancing in the portal venous and late phases in all three modalities with a central scar showing enhancement in the late phases (→**Fig. 3**).<sup>10</sup> FNH is therefore often termed “stealth” lesion because other than the arterial postcontrast phase, it may appear similar to the surrounding liver parenchyma on imaging modalities.<sup>9</sup> Additionally, a characteristic “spoke wheel” pattern of centrifugal fill-in may be seen on real-time CEUS images.

The hallmark feature is retention of contrast in the HBP while using hepatobiliary MRI contrast agents. Recently, however, four types of uptake have been documented with use of hepatocyte-specific contrast agents: (1) homo-

geneously hyperintense, (2) heterogeneously hyperintense, (3) homogeneously isointense, and (4) hypointense with peripheral ring uptake. This feature of contrast retention in the HBP is, however, not specific and may be seen in intrahepatic cholangiocarcinomas (targetoid pattern) and well-differentiated HCCs.

Atypical imaging features of FNH include size >10 cm, presence of intralesional fat, calcification typically in the central scar, absence of APHE, and signal hypointensity in the HBP.

HCA is the most important differential of FNH since it occurs in the same demographics and also shows APHE.<sup>8,9</sup> Differentiation is of paramount importance since HCAs are at risk of malignant transformation and bleeding.  $\beta$ -catenin and inflammatory subtype HCA may show a central scar and enhancement in the HBP, which can add to the diagnostic confusion.<sup>9</sup> Distinguishing features are highlighted in →**Table 2**.

Another important differential to consider is the fibrolamellar variant of HCC, which also shows arterial phase hyperenhancement and a central stellate scar. The central scar of fibrolamellar HCC, however, shows calcification and is typically T2 hypointense in contrast to FNH, which is typically T2 hyperintense. Additionally, a fibrolamellar HCC does not show uptake with hepatocyte-specific contrast agents.<sup>13</sup>

FNH-like nodules may be seen in alcoholic liver disease, postchemotherapy, and hepatic vascular diseases like

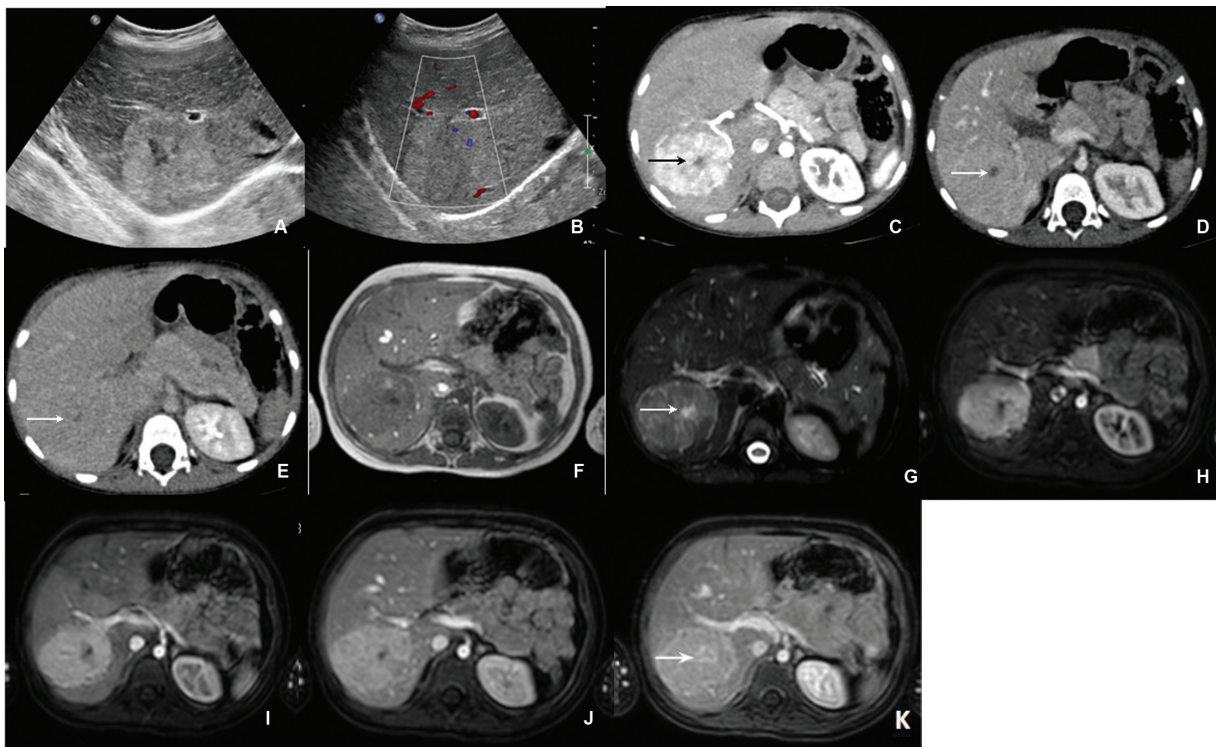


**Fig. 3** Focal nodular hyperplasia in a 17-year-old adolescent girl with incidentally detected liver mass on ultrasonography (USG). Grayscale ultrasound image shows (A) a lobulated hyperechoic mass in the right lobe with an irregular central hypoechogenicity and (B) mild vascularity on doppler. Arterial phase axial CECT image shows (C) a circumscribed avidly enhancing mass in segments VII and VI, which appears iso- to mildly hyperenhancing on (D) portal venous and (E) delayed phases. An irregular central nonenhancing component is also seen on all phases (arrows) showing mild delayed enhancement, suggestive of scar. The lesion is (F) hypointense on T1 and (G) mildly hyperintense on fat-suppressed T2-weighted images with an irregular central hyperintensity representative of the scar (arrow). (H) Nonrim arterial hyperenhancement is observed and the lesion remains mildly hyperintense on (I) portal venous and (J) hepatic venous phases. (K) There is enhancement of the central scar in the delayed phase (arrow).

**Table 2** Radiological features to distinguish hepatocellular adenomas and focal nodular hyperplasia on multiparametric magnetic resonance imaging (MRI)

Feature	Hepatocellular adenoma	Focal nodular hyperplasia
<b>Noncontrast features</b>		
1. Heterogeneity	Heterogeneous due to hemorrhage and necrosis	Relatively homogeneous
2. T1-weighted image	Varies with subtype; hyperintense due to hemorrhage; signal drop in T1-opposed phase in hepatocyte nuclear factor 1 alpha (HNF-1 $\alpha$ ) variety	No specific features in typical lesions; hypointense
3. T2-weighted image	No specific features	Stellate hyperintense central scar
<b>Postcontrast imaging</b>		
4. Type of arterial phase hyperenhancement	Typically heterogeneous nonrim APHE	Homogenous nonrim APHE with a large central feeding artery
5. Delayed phase	Absent scar	Enhancement of the central stellate scar
6. Uptake of contrast on hepatobiliary phase (most reliable)	Absent	Present

Abbreviations: APHE, arterial phase hyperenhancement.

extrahepatic portal venous obstruction (EHPVO) and Abernethy malformations.<sup>9</sup> These are identical to FNH on imaging and histology but occur in the background of inflow, outflow, and microvascular-related disturbances. FNH-like lesions are typically multiple, small, and peripheral. They may show washout in the venous phase; therefore, ancillary features like T2 hyperintensity, restricted diffusion, and growth on serial MRs have to be relied upon to differentiate from HCCs.

### Regenerative Nodules

Hepatocellular nodules are frequently seen in cirrhosis and other chronic liver disorders like Budd–Chiari syndrome and are broadly categorized into regenerative and dysplastic nodules.<sup>14,15</sup> Inciting stimuli for formation of such nodules possibly include modified circulation and inflammation.<sup>15</sup>

Regenerative nodules can be classified on the basis of size into micronodules (<3 mm) or macronodules ( $\geq$ 3 mm). In addition, large nodules with sizes up to 5 cm have also been documented in the literature.<sup>16</sup>

The lesions may show increased echogenicity on US or diffusely heterogeneous liver parenchyma. A characteristic finding of a thin hyperechoic rim surrounding the iso- to hypoechoic lesions thereby resembling a “coral reef atoll” has also been described on grayscale US and is referred to as the “atoll sign.”<sup>17</sup>

On unenhanced CT, the lesions are isodense. APHE is not seen and the lesions appear iso- to mildly hyperdense on the portal/venous and delayed phases.<sup>15,16</sup> The surrounding fibrotic strands may be identified, making these lesions more conspicuous in the later phases.

On MRI, regenerative nodules are seen as sharply circumscribed low signal intensity lesions within the liver parenchyma on unenhanced T2- and T2\*-weighted images, with variable signals on T1-weighted images. Lipid-containing regenerative nodules in addition may display signal loss in out-of-phase GRE images in comparison with the in-phase

images.<sup>16</sup> Appearance on CE MRI demonstrates features similar to CT in routine phases.

Hepatocellular-specific agents have been demonstrated to improve the accuracy to distinguish regenerative from dysplastic nodules. Since the uptake and excretion of such agents is retained in regenerative nodules, they typically enhance to the same degree as the adjacent liver in the HBP, thereby resulting in a homogeneous appearance.<sup>14</sup> Regenerative nodules possessing sufficient hepatocellular uptake but not excretory function show a hyperintense signal.

Since most regenerative nodules retain a phagocytic function, they are superparamagnetic iron oxide (SPIO) avid and appear hypointense on SPIO-enhanced T2- and T2\*-weighted images.<sup>16</sup>

With respect to size, nodules with a diameter of more than 15 mm at imaging have an increased likelihood of being dysplastic or malignant. However, preserved uptake in the HBP and SPIO retention on T2 and T2\* phases suggest benignity.<sup>16</sup> Differentiating features in between regenerative and dysplastic nodules and small HCCs are presented in **► Table 3** (**► Fig. 4**).

### Tumors of Cholangiocellular Origin

These tumors originate from the biliary epithelium and usually do not communicate with the biliary tree. Benign tumors included in this category are simple cysts, hamartomas and peribiliary cysts, and borderline lesions are mucinous cystic neoplasms (MCNs).

### Hepatic Cysts

Hepatic cysts are commonly encountered benign developmental cystic lesions of the liver and present in 2.5% of the population.<sup>18</sup> They originate from hamartomatous tissue, are lined by the biliary epithelium, and contain serous fluid.<sup>19</sup> Despite the origin, they have no communication with the biliary tree. They can be solitary or multiple, the latter being

**Table 3** Magnetic resonance (MR) features to distinguish regenerating nodules from dysplastic nodules and hepatocellular carcinoma (HCC)

Feature	Regenerative nodule	High-grade dysplastic nodule	Hepatocellular carcinoma
<b>Noncontrast imaging</b>			
1. T1-weighted image	Iso- to hyperintense	Iso- to hyperintense	Hypointense; hyperintense in cases of intralesional fat
2. T2-weighted image	Iso- to hypointense	Iso- to hypointense	Characteristically hyperintense
<b>Postcontrast imaging</b>			
3. Arterial phase hyperenhancement	Absent	Present; nonrim	Present; nonrim
4. Washout in portal venous/delayed phase	Typically iso- to hyperintense on both phases	Absent	Present
5. Uptake of contrast on hepatobiliary phase	Present; with consequent homogeneous appearance of the liver	Absent	Absent

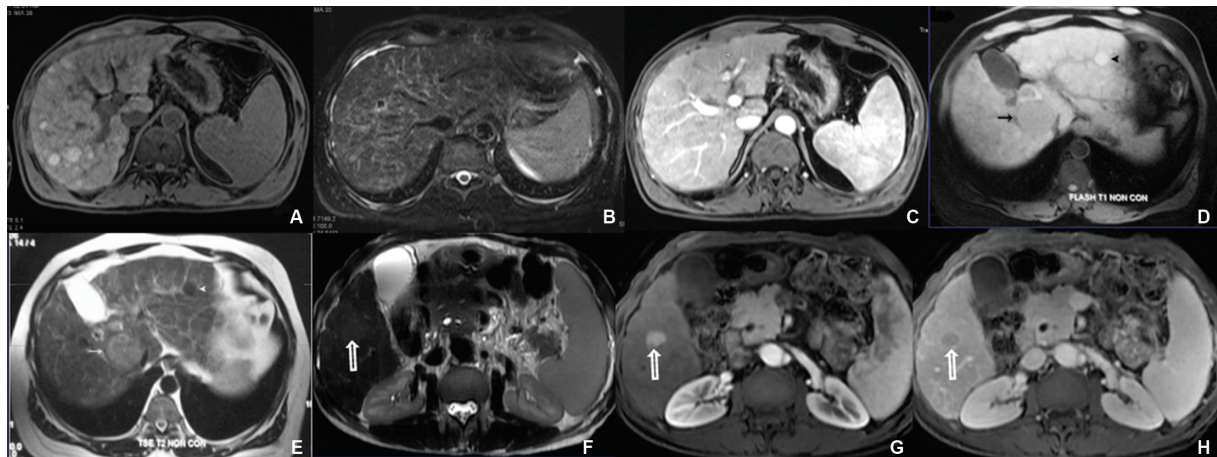


**Fig. 4** Multiple regenerative nodules in the background of cirrhosis. (A) Axial T1WI image showing multiple T1 hyperintense, which are isointense on (B) T2-weighted image (T2WI) and (C) isointense on postcontrast late arterial phase images. (D,E) Siderotic nodule and HCC coexisting in a 54-year-old male patient with alcoholic cirrhosis. (D) Axial T1 and (E) T2 W images show a siderotic nodule (arrow heads, D and E) in left lobe appearing hyperintense on T1WI and hypointense on T2WI. HCC (closed arrow) in segment VIII in contrast shows hyperintense signal on T2WI with hypointensity on T1WI. (F-H) Small hepatocellular carcinoma in a 57-year-old male patient with cirrhosis. (F) Axial T2 image shows a relatively iso-/hyperintense on T2WI with (G) non rim arterial phase hyperenhancement and (H) washout with enhancing capsule on portovenous phase images.

common. On US, they are well-defined round or oval anechoic lesions with posterior acoustic enhancement. They are homogeneously hypoattenuating on the NCCT with no enhancement on postcontrast images.<sup>18</sup> At MRI, these are homogeneously low signal on T1 and very high signal on T2W images owing to their fluid content and no enhancement on postcontrast images (►Fig. 5).<sup>18</sup> Simple cysts may get rarely complicated by intracystic hemorrhage, which shows hyperintensity on both T1-weighted and T2W images and fluid–fluid levels. Multiple hepatic cysts are seen in polycystic liver disease, an autosomal dominant disorder often found in association with autosomal dominant polycystic kidney disease.<sup>19</sup> Intracystic hemorrhagic complications are more frequently encountered in polycystic liver disease than in simple hepatic cysts.<sup>18</sup>

#### Bile Duct Hamartomas

Bile duct hamartomas, also known as von Meyenburg complexes, result from failure of involution of embryonic bile ducts. They are asymptomatic and incidentally detected on imaging, laparotomy, or autopsy. They appear as tiny hyper-echoic lesions with comet tail echoes on USG<sup>20</sup>; the anechoic cystic appearance may be difficult to appreciate. On CT, multiple small hypoattenuating cyst like lesions can be observed in both lobes of the liver.<sup>21,22</sup> In contrast to simple hepatic cysts, bile duct hamartomas are much more numerous, in both liver lobes, smaller and uniform in size (<1.5 cm), and irregular in outline. Usually, no appreciable enhancement is seen; however, some mural nodular enhancement may be seen.<sup>23</sup> In magnetic resonance cholangiopancreatography (MRCP) images, they appear as small

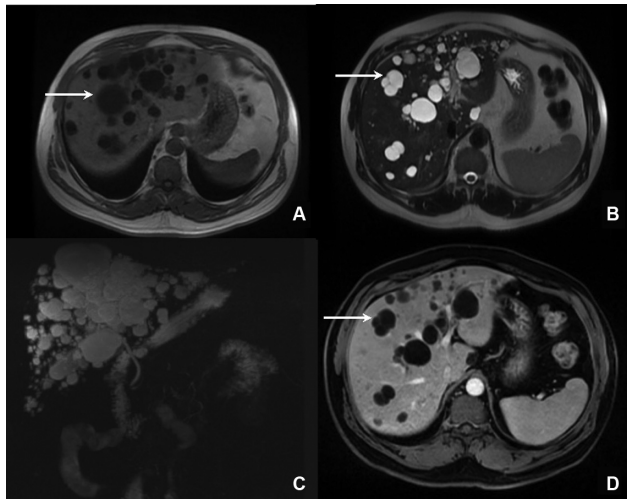


**Fig. 5** Multiple simple liver cysts in a 42-year-old man with polycystic liver disease. Axial (A) T1-weighted image (arrow), (B) T2-weighted image (arrow), and (C) coronal thick maximal intensity projection (MIP) magnetic resonance cholangiopancreatography (MRCP) images show multiple thin-walled cysts showing (D) homogeneously low T1 signal and high T2 signal with no enhancement on axial postcontrast image.

cystic lesions without any communication with the biliary tree (►Fig. 6).

#### Peribiliary Cysts

Peribiliary cysts are cystic dilatation of the bile duct glands that are usually associated with cirrhosis and portal hypertension. Commonly, these cysts occur in the large central ducts and near the hepatic hilum. These are benign cysts; however, rarely bile duct obstruction can be seen due to large cysts.<sup>24</sup> In the US, rounded or tubular anechoic structures are seen along the portal tracts, findings that may be mistaken for dilated bile ducts.<sup>25</sup> Similarly, hypoattenuating cystic structures are seen on CT and hyperintense cystic structures are seen on T2W MR images in periportal locations (►Fig. 7).<sup>26</sup>

#### Mucinous Cystic Neoplasm of the Liver

Mucinous cystic neoplasms (MCNs), formerly known as biliary cystadenomas, are rare cystic mucinous neoplasms of the liver. They are benign, but there is a high risk (20–23%) of transformation to invasive cancer.<sup>27</sup> The lesions are vari-

able in size and large lesions up to 35 cm have been reported with almost exclusive involvement of the left hepatic lobe.<sup>28</sup> They have been found to have ovarian stroma on histopathological analysis.<sup>28</sup> On imaging, MCNs are cystic, multilocular with multiple internal septations and mural nodularity.<sup>28</sup> These thin septations exhibit enhancement on postcontrast images, which tends to be smooth and regular (►Fig. 8). Distinction between benign and malignant MCN-L remains difficult on imaging, although features like irregular thick septal enhancement, calcifications, and mural nodularity suggest the presence of the latter.<sup>29,30</sup> The role of serum tumor markers such as carcinoembryonic antigen (CEA) and cancer antigen 19–9 (CA 19–9) remains limited for differentiation, with the levels ranging from marked elevation to normal in invasive carcinoma.<sup>31</sup> CEA and CA 19–9 levels in cyst fluid also have limited utility for differentiating MCN from non-neoplastic entities.<sup>32</sup> Imaging findings requiring sampling include mural nodules, wall enhancement, and calcifications as these have been found to be significantly associated with malignancy on surgical exploration.<sup>31</sup>

The two major differential diagnoses include complicated simple cysts and hydatid cysts. Simple cysts usually lack or have thin incomplete nonenhancing septations and are often multiple, which allows a fairly confident diagnosis.<sup>33</sup> While hydatid cysts preferentially affect the right lobe, a lesion within the left liver is more suggestive of benign MCN. Mural or septal calcifications, a multicystic honeycomb pattern (due to multiple daughter cysts), and visualization of membranes of broken daughter vesicles, which appear as “serpentine linear structures” within the cyst, are the specific features of hydatid disease.<sup>33</sup>

#### Tumors of Mesenchymal Origin

This category incorporates lesions originating from the hepatic stromal elements. The most common lesion incorporated is hemangioma along with rarer neoplasms like lipoma, angiomyolipomas (AMLs), paragangliomas, and pseudotumors.

#### Hemangiomas

Hemangiomas comprise the most frequent benign liver lesions and are commonly detected incidentally. These lesions consist of blood-filled vascular spaces and hence are classified under low-flow vascular malformations as per the latest International

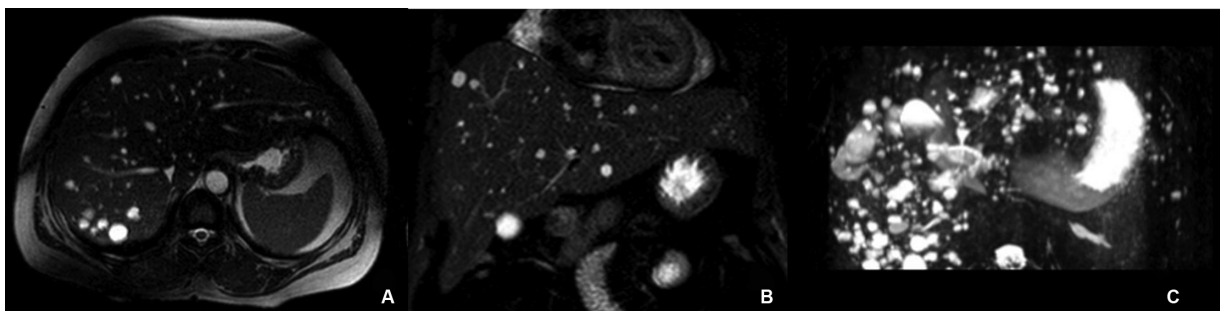


**Fig. 6** Incidentally detected multiple biliary hamartomas. (A) Axial and (B) coronal T2-weighted images show multiple small round similar-sized cystic lesions in both lobes in peripheral predominant location with no biliary communication on (C) the magnetic resonance cholangiopancreatography (MRCP) image.



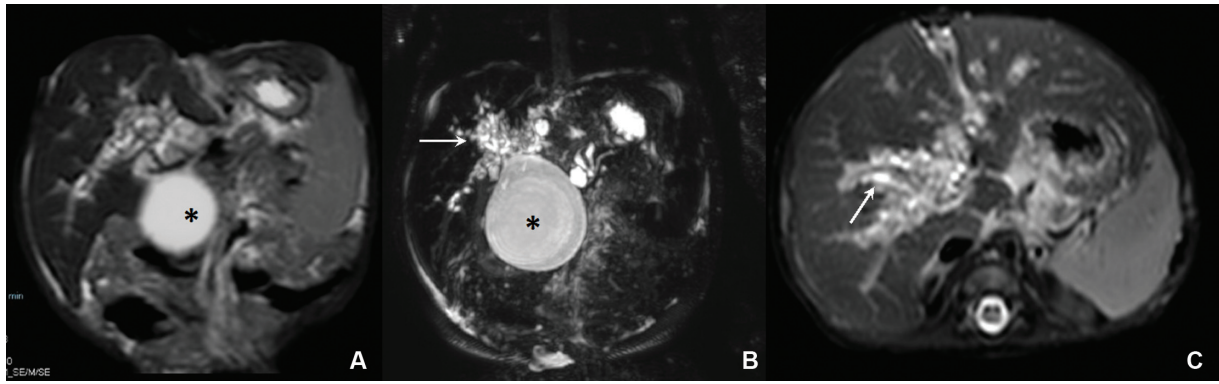


**Fig. 7** Peribiliary cysts in a pediatric patient with type I choledochal cyst. (A) Coronal T2-weighted and (B) magnetic resonance cholangiopancreatography (MRCP) images show saccular dilatation of CBD (*asterisks*) with multiple tiny round to tubular hyperintense cysts (*arrows*) in both lobes, which are preferentially located along the portal tracts (B,C), but do not appear to communicate with the biliary tree.

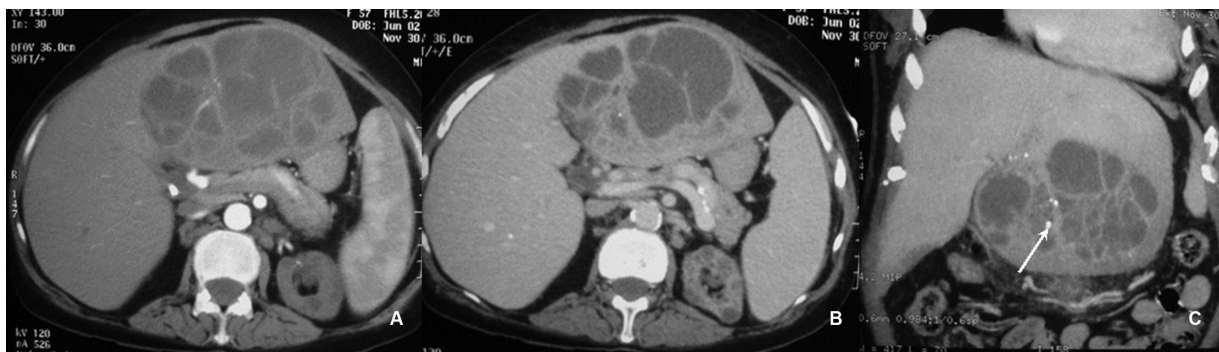


**Fig. 8** Mucinous cystic neoplasm of the liver (MCN-L) in a 40-year-old woman. Axial contrast-enhanced computed tomography (CECT) images in (A) arterial and (B) venous phases show a large multiloculated cystic lesion with multiple enhancing septations occupying and expanding the left lobe of the liver. (C) Coronal postcontrast image in venous phase shows few punctate calcifications (*arrows*) within the lesion. Diagnosis was subsequently confirmed post resection.

Society for the Study of Vascular Anomalies (ISSVA) guidelines.<sup>34</sup> Hemangiomas can have varied presentations on imaging and have been broadly categorized into typical and atypical forms. In addition; they can be categorized on the basis of size criteria into small (<1.5 cm), medium (1.5–5 cm), and large (>5 cm).<sup>35</sup> Lesions greater than 10 cm are termed as giant hemangiomas.

#### Typical Hemangiomas

These lesions are typically less than 3 cm in size and consists of mainly two types: cavernous and flash-filling hemangiomas.

#### Cavernous Hemangiomas

Such hemangiomas are so called as they contain multiple cavernous vascular spaces in histology. They appear as homogeneously hyperechoic lesions on US and demonstrate posterior acoustic enhancement.<sup>31,32</sup> The echogenicity is attributed to the cavernous spaces acting as multiple interfaces due to intervening fibrous stroma, thereby leading to multiple reflections. In addition, there is apparent continuous movement of the speckled echogenicity within the lesion on US, a phenomenon known as the “fluttering sign.”<sup>36</sup> A lesion can be confidently diagnosed as hemangioma on US if it is well defined, homogeneously echogenic, less than 3 cm, and in the absence of cirrhosis or any malignancy.<sup>35</sup>

On NCCT, cavernous hemangiomas (CHs) typically remain isodense to the liver vessels. Postcontrast injection, they show a characteristic pattern of peripheral nodular discontinuous enhancement, which shows similar density as that of the blood pool in all the phases (► **Fig. 9**).<sup>37</sup> There is progressive centripetal fill-in, which may even become complete in the delayed phase. However, sometimes a complete fill-in of CHs may require even more than 15 minutes on CT and MR examinations. A similar pattern of enhancement is observed in CEUS.<sup>37</sup>

As for all hepatic lesions, MRI remains the imaging modality of choice for hemangiomas with the lesions showing a homogeneously high signal similar to that of cerebrospinal fluid (CSF) on T2W images, known as “light bulb sign” and lobulated margins. They remain hypointense on T1 and do not demonstrate diffusion restriction (► **Fig. 10**).<sup>35,38</sup> The MRI enhancement pattern using an extracellular contrast agent is identical to that of the CT, that is, peripheral nodular enhancement and progressive centripetal fill-in (► **Fig. 10**). Sometimes a “pseudo-washout” pattern has been observed on the 3-minute transitional phase with the use of Gd-EOB-DTPA (gadoxetate; trade name: Eovist) as the hepatocyte-specific contrast agent, which may lead to a misdiagnosis.<sup>35</sup> This occurs due to fast pharmacokinetics of gadoxetate disodium, with its early washout from the vascular spaces

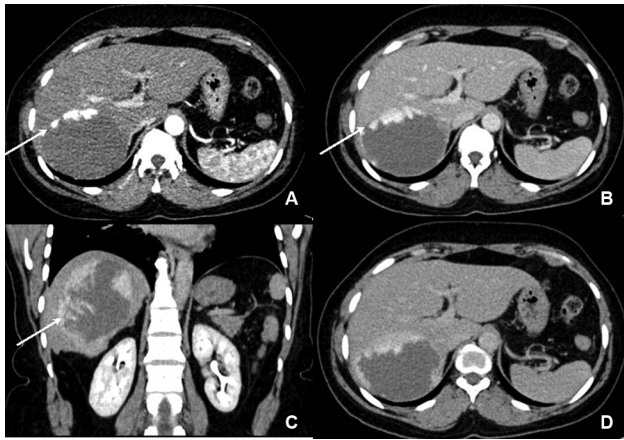


**Fig. 9** Incidentally detected large hemangioma in a 36-year-old woman. Axial CECT image in (A) the arterial phase shows a well-marginated lesion in segment VII of the right lobe, which demonstrates a characteristic discontinuous peripheral nodular enhancement (arrow) with progressive centripetal fill-in on (B,C) portal venous (arrows) and (D) delayed phases. The enhancement pattern parallels that of blood pool (observed by enhancement of the aorta) on all phases.

of the CH and increased enhancement of the surrounding liver parenchyma. As hemangiomas do not contain hepatocytes, they appear hypointense in the HBP.<sup>39</sup>

#### Flash-Filling Hemangiomas

Also known as rapidly filling or capillary hemangiomas, flash-filling hemangiomas (FFHs) present as small lesions (<1.5 cm) and shows prompt, avid, and homogeneous enhancement in the arterial phase on CT/MRI with a density/intensity equivalent to that of the aorta during all dynamic phases (►**Fig. 11**). A “pseudo-washout” in the delayed phase in hepatobiliary MRI using Gd-EOB-DTPA can also be observed. FFHs are associated with an arterio-

portal shunt and transient perilesional enhancement, which is attributed to perfusion abnormalities, also known as transient hepatic enhancement difference (THED).<sup>35,39</sup>

#### Atypical Hemangiomas

Hemangiomas occasionally may not display the classically mentioned enhancement characteristics, and it is imperative to recognize these lesions for formulating the correct diagnosis.<sup>38</sup> One such example includes sclerosed hemangioma (SH), also known as thrombosed or hyalinized hemangioma. These lesions are consequent to degeneration and consist of extensive fibrous tissue, which leads to obliteration of the vascular spaces. The fibrosis typically begins in the center of the lesion and can involve the entire hemangioma.<sup>35,38</sup> These lesions appear as irregular heterogeneous masses on US, CT, and MRI with loss of T2 hyperintensity on MR owing to the fibrosis. In the arterial phase, the lesions display slight rim enhancement with occasional nonperipheral nodular enhancement, which may persist in the venous phase, thus appearing as bright dots within the hypodense/hypointense lesion that has also been referred to as the “bright dot sign.”<sup>40</sup> Contrary to the typical counterparts, SHs demonstrate slow progressive fill-in and may remain nonenhancing several hours postcontrast administration.<sup>35,38</sup>

Other features of SHs include volume loss, capsular retraction, and wedge-shaped regions of THED in the surrounding parenchyma on CT and MRI. Although the diagnosis of SH may be suggested, histological proof is often necessary. Common differentials include hypovascular lesions including metastases and cholangiocarcinoma.<sup>35</sup>

#### Angiomyolipoma

These rare benign tumors subgrouped under the umbrella category of perivascular epithelioid cell tumors (PEComas) are composed of smooth muscles with blood vessels and

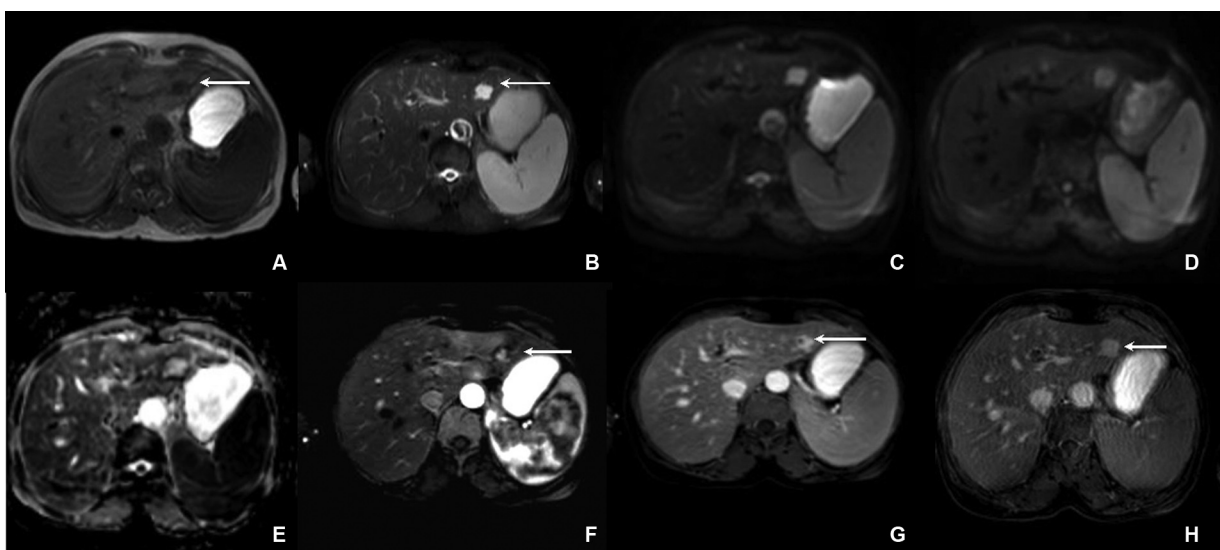


**Fig. 10** Magnetic resonance (MR) features of hemangioma. (A) Axial T1 and (B) T2-weighted images show a lobulated T1 hypointense and T2 hyperintense lesion in segment III of the left lobe (arrows) which remains bright on (C) diffusion weighted imaging (DWI; b-value: 0). The lesion remains bright on (D) high b-value image (b-value: 400) and (E) corresponding apparent diffusion coefficient (ADC) image suggesting T2 shine through effect. Axial postcontrast images in (F) arterial, (G) portal venous, and (H) delayed phases demonstrate characteristic nodular enhancement with complete fill-in of the lesion in the delayed phase (arrows).

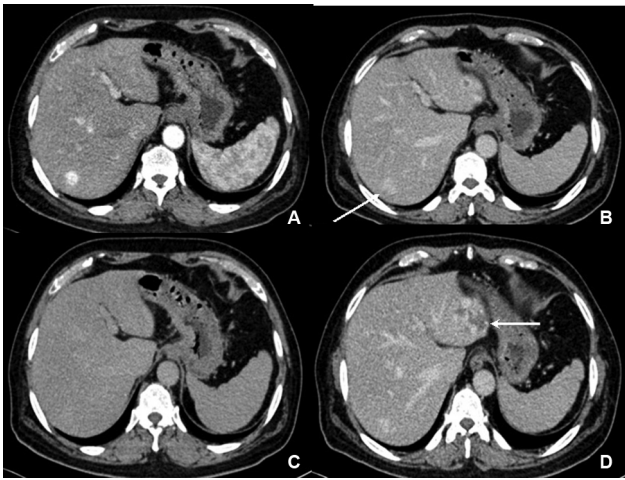


**Fig. 11** Flash filling hemangioma. Axial contrast-enhanced computed tomography (CECT) image in the (A) arterial phase shows a small well-margined lesion in segment VII with avid homogeneous enhancement (arrow), which persists in the (B) portal venous phase. (C) The lesion is masked on delayed phase due to similar enhancement with the rest of the liver parenchyma. Also, the degree of enhancement matches with that of vessels. (D) Axial CECT image in the portal venous phase at a caudal section demonstrates another hemangioma in segment III (arrow).

adipose tissue. Most occur sporadically; however, an association with tuberous sclerosis is well documented.<sup>1</sup>

On US, hepatic AMLs appear as circumscribed hyperechoic lesions and therefore simulate hemangiomas. They may show subtle shadowing and are generally hypervascular on Doppler imaging.<sup>41</sup>

CT demonstrates areas of macroscopic fat with marked enhancement and visualization of large central vessels in the arterial phase. In MRI, macroscopic fat may be detected by using fat suppression techniques, based on the distribution and degree of adipose tissue.<sup>1</sup> Imaging with in-phase and opposed-phase gradient echo T1-weighted sequences helps in detection of microscopic fat.<sup>1,41</sup> The T2 signal and enhancement pattern is determined by the relative proportion of the epithelioid (angiomatous) and myomatous elements.<sup>42,43</sup> Hypervascular epithelioid components show high T2 signal with intense APHE and venous phase washout. In contrast, the myomatous components remain T2 hypointense and hypoenhancing in the arterial phase and there is progressive

enhancement in the venous and delayed phases.<sup>42</sup> The presence of an early draining hepatic vein points toward the diagnosis of AML. In the HBP, the tumor is usually hypointense with variable diffusion restriction on DWI.<sup>44</sup>

### Lipoma

Although lipomas are rarely encountered in the liver, they typically do not represent a diagnostic challenge due to typical CT and MR features. On US, hepatic lipomas are seen as well-circumscribed echogenic lesions with or without acoustic shadowing (► Fig. 12). Lipomas in the liver are homogeneously hypoattenuating on CT and do not show enhancement on postcontrast images (► Fig. 11).<sup>1</sup> MRI shows bulk fat within the lesion using fat suppression techniques.<sup>1</sup>

### Paraganglioma

Paragangliomas represent rare tumors of neural crest origin and are generally benign. They are typically seen along the sympathetic chain; however, numerous intra-abdominal locations have been described, including the liver. Just like the majority of mesenchymal tumors, they show nonspecific imaging characteristics on CT and MRI.<sup>45</sup> On CT, they appear as smooth, well-circumscribed lesions with avid contrast enhancement and occasional cystic areas and punctate calcifications.<sup>1,45</sup> MRI demonstrates high signal intensity as compared with the surrounding liver on T2W images with intervening hypointense internal septa and avid enhancement after contrast administration.<sup>45</sup>

### Inflammatory Pseudotumor

Inflammatory pseudotumor or inflammatory myofibroblastic tumor is a benign hepatic tumor composed of inflammatory cells and fibrous stroma.<sup>46</sup> On US, the lesions may appear hypo- or hyperechoic with increase through transmission and multiple septa.<sup>1</sup> The lesions may be homogeneous or heterogeneous on CT. They are hypoattenuating to liver parenchyma on noncontrast images with varying patterns of enhancement.<sup>47</sup> Generally, they show mild, irregular hypoenhancement in the arterial phase with delayed enhancement in the portal venous or delayed phases, which is reflective of the fibrotic nature of these tumors.<sup>47,48</sup> A peripheral enhancement pattern with multiple internal septations has also been described.<sup>46,49</sup> Coarse calcification and capsular retraction are other documented features. MRI

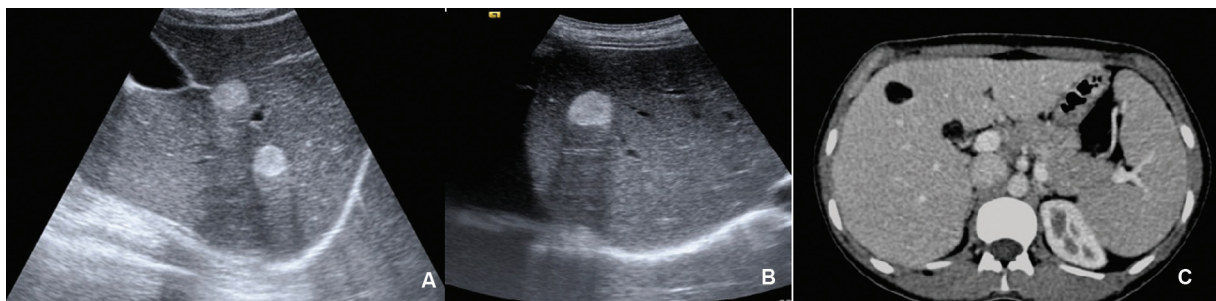


**Fig. 12** Multiple liver lipomas. (A,B) Grayscale ultrasound images show multiple well-circumscribed homogeneously hyperechoic hepatic lesions that show diffuse fat attenuation on the (C) corresponding axial contrast-enhanced computed tomography (CECT) image.



**Fig. 13** (A) Approach to a solid hepatic mass on magnetic resonance imaging (MRI). (B) Approach to solid mass with nonrim arterial phase hyperenhancement (APHE). (C) Approach to a cystic hepatic mass on MRI. \*For a solid mass with nonrim APHE, refer to **Fig. 13b**.

appearance includes T1 and T2 hypointensity owing to the presence of fibrosis with enhancement in the delayed-phase postgadolinium administration.<sup>49</sup>

## Conclusion

Benign liver tumors are classified on the basis of their cell of origin into hepatocellular, cholangiocellular, and mesenchymal tumors. Systematic evaluation of the enhancement characteristics on cross-sectional imaging can help the radiologist reach the proper diagnosis. An algorithmic approach on CEMRI may assist in achieving this as has been described in ► **Fig. 13.**

### Funding

None.

### Conflict of Interest

None declared.

## References

- Anderson SW, Kruskal JB, Kane RA. Benign hepatic tumors and iatrogenic pseudotumors. *Radiographics* 2009;29(01):211–229
- Tao LC. Oral contraceptive-associated liver cell adenoma and hepatocellular carcinoma. Cytomorphology and mechanism of malignant transformation. *Cancer* 1991;68(02):341–347
- Foster JH, Berman MM. The malignant transformation of liver cell adenomas. *Arch Surg* 1994;129(07):712–717
- Nault JC, Couchy G, Balabaud C, et al; GENTHEP Investigators. Molecular classification of hepatocellular adenoma associates with risk factors, bleeding, and malignant transformation. *Gastroenterology* 2017;152(04):880–894.e6
- Zulfiqar M, Sirlin CB, Yoneda N, et al. Hepatocellular adenomas: understanding the pathomolecular lexicon, MRI features, terminology, and pitfalls to inform a standardized approach. *J Magn Reson Imaging* 2020;51(06):1630–1640
- Garcovich M, Faccia M, Meloni F, et al. Contrast-enhanced ultrasound patterns of hepatocellular adenoma: an Italian multicenter experience. *J Ultrasound* 2019;22(02):157–165
- Nguyen BN, Fléjou JF, Terris B, Belghiti J, Degott C. Focal nodular hyperplasia of the liver: a comprehensive pathologic study of 305 lesions and recognition of new histologic forms. *Am J Surg Pathol* 1999;23(12):1441–1454
- Wanless IR, Mawdsley C, Adams R. On the pathogenesis of focal nodular hyperplasia of the liver. *Hepatology* 1985;5(06):1194–1200
- Mortelé KJ, Praet M, Van Vlierberghe H, Kunnen M, Ros PRCT. CT and MR imaging findings in focal nodular hyperplasia of the liver: radiologic-pathologic correlation. *AJR Am J Roentgenol* 2000;175(03):687–692
- D'Onofrio M, Crosara S, De Robertis R, Canestrini S, Mucelli RP. Contrast-enhanced ultrasound of focal liver lesions. *AJR Am J Roentgenol* 2015;205(01):W56–66
- Ronot M, Paradis V, Duran R, et al. MR findings of steatotic focal nodular hyperplasia and comparison with other fatty tumours. *Eur Radiol* 2013;23(04):914–923
- Semelka RC, Martin DR, Balci C, Lance T. Focal liver lesions: comparison of dual-phase CT and multisequence multiplanar MR imaging including dynamic gadolinium enhancement. *J Magn Reson Imaging* 2001;13(03):397–401
- Ganeshan D, Szklaruk J, Kundra V, Kaseb A, Rashid A, Elsayes KM. Imaging features of fibrolamellar hepatocellular carcinoma. *AJR Am J Roentgenol* 2014;202(03):544–552
- Brancatelli G, Federle MP, Grazioli L, Golfieri R, Lencioni R. Benign regenerative nodules in Budd-Chiari syndrome and other vascular disorders of the liver: radiologic-pathologic and clinical correlation. *Radiographics* 2002;22(04):847–862
- Brancatelli G, Federle MP, Grazioli L, Golfieri R, Lencioni R. Large regenerative nodules in Budd-Chiari syndrome and other vascular disorders of the liver: CT and MR imaging findings with clinicopathologic correlation. *AJR Am J Roentgenol* 2002;178(04):877–883
- Hanna RF, Aguirre DA, Kased N, Emery SC, Peterson MR, Sirlin CB. Cirrhosis-associated hepatocellular nodules: correlation of histopathologic and MR imaging features. *Radiographics* 2008;28(03):747–769
- Caturelli E, Ghittoni G, Ranalli TV, Gomes VV. Nodular regenerative hyperplasia of the liver: coral atoll-like lesions on ultrasound are characteristic in predisposed patients. *Br J Radiol* 2011;84(1003):e129–e134
- Mathieu D, Vilgrain V, Mahfouz AE, Anglade MC, Vullierme MP, Denys A. Benign liver tumors. *Magn Reson Imaging Clin N Am* 1997;5(02):255–288
- vanSonnenberg E, Wroblecka JT, D'Agostino HB, et al. Symptomatic hepatic cysts: percutaneous drainage and sclerosis. *Radiology* 1994;190(02):387–392
- Zheng RQ, Zhang B, Kudo M, Onda H, Inoue T. Imaging findings of biliary hamartomas. *World J Gastroenterol* 2005;11(40):6354–6359
- Martinoli C, Cittadini G Jr, Rollandi GA, Conzi R. Case report: imaging of bile duct hamartomas. *Clin Radiol* 1992;45(03):203–205
- Wohlgemuth WA, Böttger J, Bohndorf K. MRI, CT, US and ERCP in the evaluation of bile duct hamartomas (von Meyenburg complex): a case report. *Eur Radiol* 1998;8(09):1623–1626
- Mortelé KJ, Ros PR. Cystic focal liver lesions in the adult: differential CT and MR imaging features. *Radiographics* 2001;21(04):895–910
- Seguchi T, Akiyama Y, Itoh H, et al. Multiple hepatic peribiliary cysts with cirrhosis. *J Gastroenterol* 2004;39(04):384–390
- Terayama N, Matsui O, Hoshiba K, et al. Peribiliary cysts in liver cirrhosis: US, CT, and MR findings. *J Comput Assist Tomogr* 1995;19(03):419–423
- Motoo Y, Yamaguchi Y, Watanabe H, Okai T, Sawabu N. Hepatic peribiliary cysts diagnosed by magnetic resonance cholangiography. *J Gastroenterol* 2001;36(04):271–275
- Zen Y, Pedica F, Patcha VR, et al. Mucinous cystic neoplasms of the liver: a clinicopathological study and comparison with intra-ductal papillary neoplasms of the bile duct. *Mod Pathol* 2011;24(08):1079–1089
- Buetow PC, Buck JL, Pantongrag-Brown L, et al. Biliary cystadenoma and cystadenocarcinoma: clinical-imaging-pathologic correlations with emphasis on the importance of ovarian stroma. *Radiology* 1995;196(03):805–810
- Lewin M, Mourra N, Honigman I, et al. Assessment of MRI and MRCP in diagnosis of biliary cystadenoma and cystadenocarcinoma. *Eur Radiol* 2006;16(02):407–413
- Lee MH, Katabathina VS, Lubner MG, et al. Mucin-producing cystic hepatobiliary neoplasms: updated nomenclature and clinical, pathologic, and imaging features. *Radiographics* 2021;41(06):1592–1610
- Klompouhouwer AJ, Ten Cate DWG, Willemssen FEJA, et al. The impact of imaging on the surgical management of biliary cystadenomas and cystadenocarcinomas; a systematic review. *HPB (Oxford)* 2019;21(10):1257–1267
- Choi HK, Lee JK, Lee KH, et al. Differential diagnosis for intrahepatic biliary cystadenoma and hepatic simple cyst: significance of cystic fluid analysis and radiologic findings. *J Clin Gastroenterol* 2010;44(04):289–293
- Tholomier C, Wang Y, Aleynikova O, Vanounou T, Pelletier JS. Biliary mucinous cystic neoplasm mimicking a hydatid cyst: a case report and literature review. *BMC Gastroenterol* 2019;19(01):103

- 34 Wassef M, Blei F, Adams D, et al; ISSVA Board and Scientific Committee. Vascular anomalies classification: recommendations from the international society for the study of vascular anomalies. *Pediatrics* 2015;136(01):e203–e214
- 35 Mamone G, Di Piazza A, Carollo V, et al. Imaging of hepatic hemangioma: from A to Z. *Abdom Radiol (NY)* 2020;45(03):672–691
- 36 Kobayashi N, Iijima H, Tada T, et al. A new ultrasonographic “fluttering sign” for hepatic hemangioma. *Ultrasound Med Biol* 2021;47(04):941–946
- 37 Kim KW, Kim TK, Han JK, et al. Hepatic hemangiomas: spectrum of US appearances on gray-scale, power Doppler, and contrast-enhanced US. *Korean J Radiol* 2000;1(04):191–197
- 38 Vilgrain V, Boulos L, Vullierme MP, Denys A, Terris B, Menu Y. Imaging of atypical hemangiomas of the liver with pathologic correlation. *Radiographics* 2000;20(02):379–397
- 39 Dane B, Shanbhogue K, Menias CO, Taffel MT. The humbling hemangioma: uncommon CT and MRI imaging features and mimickers of hepatic hemangiomas. *Clin Imaging* 2021;74:55–63
- 40 Jang HJ, Choi BI, Kim TK, et al. Atypical small hemangiomas of the liver: “bright dot” sign at two-phase spiral CT. *Radiology* 1998;208(02):543–548
- 41 Calame P, Tyrode G, Weil Verhoeven D, et al. Clinical characteristics and outcomes of patients with hepatic angiomyolipoma: a literature review. *World J Gastroenterol* 2021;27(19):2299–2311
- 42 Razik A, Malla S, Goyal A, et al. Unusual primary neoplasms of the adult liver: review of imaging appearances and differential diagnosis. *Curr Probl Diagn Radiol* 2022;51(01):73–85
- 43 Thampy R, Elsayes KM, Menias CO, et al. Imaging features of rare mesenchymal liver tumours: beyond haemangiomas. *Br J Radiol* 2017;90(1079):20170373
- 44 Tan Y, Xiao EH. Hepatic perivascular epithelioid cell tumor (PEComa): dynamic CT, MRI, ultrasonography, and pathologic features—analysis of 7 cases and review of the literature. *Abdom Imaging* 2012;37(05):781–787
- 45 Liao W, Ding ZY, Zhang B, et al. Primary functioning hepatic paraganglioma mimicking hepatocellular carcinoma: a case report and literature review. *Medicine (Baltimore)* 2018;97(17):e0293
- 46 Narla LD, Newman B, Spottswood SS, Narla S, Kolli R. Inflammatory pseudotumor. *Radiographics* 2003;23(03):719–729
- 47 Xiao Y, Zhou S, Ma C, Luo J, Zhu H, Tang F. Radiological and histopathological features of hepatic inflammatory myofibroblastic tumour: analysis of 10 cases. *Clin Radiol* 2013;68(11):1114–1120
- 48 Tang L, Lai ECH, Cong WM, et al. Inflammatory myofibroblastic tumor of the liver: a cohort study. *World J Surg* 2010;34(02):309–313
- 49 Yan FH, Zhou KR, Jiang YP, Shi WB. Inflammatory pseudotumor of the liver: 13 cases of MRI findings. *World J Gastroenterol* 2001;7(03):422–424